Automation of Aircraft Engine Fuel Controls Tests: *An Industrial Case Study involving PID Control of a Nozzle Emulator*

Ifeanyi Azolibe*, Euan W. McGookin*

**Aerospace Sciences Research Division, School of Engineering,*
University of Glasgow,
University Avenue, Glasgow G12 8QQ, U.K.
i.Azolibe.1@research.gla.ac.uk; Ifeanyi.Azolibe@yahoo.com; Euan.McGookin@glasgow.ac.uk

Keywords: *test automation, aircraft fuel control unit, PID control, pneumatic regulator, V2500 FMU*

Abstract

The test of fuel control systems used on civil aircraft engines is performed with a network of distributed and, by design, isolated systems. The co-ordination of these test systems is performed manually by human operators in order to verify the airworthiness of a fuel control system throughout the products' lifecycle. The main objective of this study is the automation of an existing network of systems for fuel control tests. The aspect of automation that is considered in this paper is the control of the engine nozzle emulator which is critical to determine the airworthiness of repaired fuel control systems. This system is realized using a model following PID controller design approach. The results from simulation studies and a hardware-in-the-loop test are presented. These demonstrate that this PID control structure provides the necessary level of accuracy and robustness for this engineering process.

1 Introduction

Fuel control systems are a critical, but less known, components of modern aircraft engines [1]. These systems are the intelligent 'taps' in aircraft engines, that ensure the right amount of fuel flows to the combustion chamber of the engine. This in turn generates the thrust and power demanded by the pilot to fulfill every stage of flight [2] . The fuel control system is in continuous use throughout taxiing, take-off, cruising, landing and shutdown. In fact the efficiency of this system impacts on the economics of flight in a significant way. During its life cycle a fuel control unit must be repaired or overhauled to sustain its efficient performance and the safe operation of the engine during flight [3].

In the context of maintenance, a test of airworthiness is performed after a fuel control system undergoes a Maintenance, Repair or Overhaul (MRO) [1]. As the volume of air travel grows, the capability to perform more tests in shorter periods of time becomes essential for maintaining a competitive aftermarket service. With forecast growth in air travel [4] [5], a lack of such capability would become a bottleneck. Therefore, the retrofit of automation to existing test systems is being used to extend their capability for the near future. In order to mitigate the impact competitive impact such bottleneck would have.

Since the test procedure and systems have been designed to aid optimal execution of tests by a human operator, the operator has to provide the feedback control necessary to drive different actuators the test rig actuators for example.

Fundamentally, the retrofit of automation to test systems required process data from different test systems for the automatic control of the actuation mechanisms for each test process. A data management architecture has been designed to drive and support the different facets of automation e.g. data acquisition and the automatic controllers for the process actuation mechanisms [1].

In this paper, the automation of the control of a nozzle emulator is presented. It is a part of the integrated automation system developed to set test conditions during the test of an aircraft fuel control system automatically. The type of fuel control that is the focus of this study is a Fuel Metering Unit (FMU), and the specific fuel control system is the V2500 FMU on the V2500 aircraft engine [6], [7].

During a test procedure, the actuation mechanism of the nozzle emulator in a test rig, Fig. 1(bottom grey box), is used to set a back pressure in the FMU. This backpressure emulates the pressure that would result inside of the FMU, through the fuel line connecting it to the nozzle on the aircraft engine. Such that its magnitude is determined by the nozzle orifice available to the metered fuel flowing from the FMU to the combustion chamber.

The main element of the automation of the control of the nozzle emulator is an electronic controller based on the PID control law [8]–[13]. It has been designed using a model following approach. Using models constructed from a daisy chain of mass-spring-damper elements, representing the actuation mechanism Fig. 1 (top grey box).

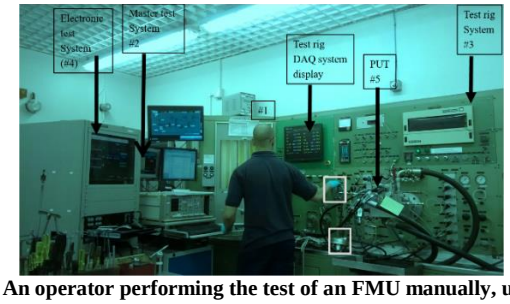

Fig. 1: An operator performing the test of an FMU manually, using the test rig and other test systems

The nozzle emulator is a hydraulic valve that is normally controlled by means of a manually operated mechanical pneumatic regulator (MPR). In order to automate its control, its actuation mechanism has been replaced with an automation capable alternative. Where this alternative required an electronic controller (implemented in software). Due to a lack of precedence in the literature, this controller had to be realized using either models or expert control systems approaches. For this study, the model-based design approach was chosen.

The development of a mathematical model that represents this system is non-trivial given the multi-disciplinary nature of each physical element i.e. from mechanical to pneumatic and then hydraulic; to electronic and hydraulic. In spite of this challenge, complete automatic control of a critical component used to test the V2500 FMU has been achieved.

Although the particular design considered here is specific to the automation of the nozzle emulator, the basic concepts are generally applicable in other areas. For example, the derivation of a tool to diagnose the faulty operation of the nozzle emulator, using the inherent controller behavior in real-time [14], [15]. Given that malfunction of the nozzle emulator usually results in the failure of tests procedures. This wastes vital production time because of time spent in troubleshooting why the process it controls cannot be set within a specified test range. Also, some aspect of the modeling concepts could be used as a start point to model pneumatic regulators for other research applications. E.g. to model [16], [17].

In the second section, a detailed introduction is given to the structure of this nozzle emulator's actuation mechanism and the process it is used to set during a test. Then how it was transformed and adapted for automation will be discussed briefly. In Section 3, the modelling of this actuation mechanism from first principles is presented. This is followed by the results of simulations, validated against data collected from the actual nozzle emulator in a test rig. The results of a hardware-in-the-loop test are presented to demonstrate automatic control of the nozzle emulator, which is an essential part of the automation of the test systems. In Section 4 the results of automatic control across the full operational range of the V2500 FMU fuel control system are presented. These have been recorded from the already installed, completely retrofitted automation system. This is analyzed and discussed, prior to the conclusions of this work in Section 5.

2 The nozzle emulator

Naturally the constriction of the nozzle orifice results in a smaller opening for the fuel to flow through. This in turn increases the backpressure in the FMU during any stage of an aircraft's flight. Similarly, when the nozzle constriction reduces, the orifice available to fuel flow increases and this reduces the backpressure. The resulting increase in fuel flow to the combustion chamber leads to an increase in the thrust generated by the engine. The metered fuel flow from the FMU is determined by the flight commands from the pilot via the position of the power lever in the cockpit [2].

The nozzle emulator is a hydraulic valve, in-line with the metered fuel flow line of the FMU, which is upstream as illustrated in the schematic diagram of Fig. 2. In the context of testing an FMU, downstream of the nozzle emulator is the fuel tank to which the test calibration fluid returns to.

To actuate the nozzle emulator, an operator applies an anti-/clockwise torque to a mechanical pneumatic regulator (MPR)—the actuation mechanism. Such that the operator continually adjusts the actuation mechanism, until the desired backpressure is achieved in the FMU. This human based closed-loop control is illustrated in Fig. 3.

A clockwise torque results in an increase in the regulated pneumatic pressure of the regulator, loaded on to the nozzle emulator.

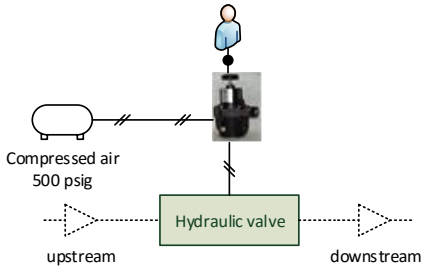

Fig. 2: Manual control structure of the nozzle emulator

This displaces the nozzle emulator's valve stem downwards, in a way that restricts the orifice available to metered fuel flow from the FMU. Thereby resulting in a proportional increase in the backpressure inside the FMU.

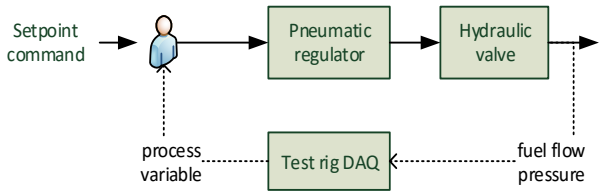

Fig. 3: The closed-loop control structure of the nozzle emulator with the operator providing feedback

While an anticlockwise torque relieves the pneumatic pressure on the emulator. This results in the emulator's valve stem moving upward due to the flow force being greater than the applied pneumatically applied force, which makes the orifice available to fuel flow larger. As a result the backpressure inside the FMU decreases, due to the smaller restriction of the nozzle emulator to metered flow from the FMU (going back to the fuel tank downstream).

3 Model-based design of PID controller

Automation of the control of the nozzle emulator can be achieved using by replacing its actuation mechanism, the MPR, with an electro-pneumatic regulator (EPR). Or replace both the MPR and the nozzle emulator with an electro-hydraulic valve (EHV).

After an analysis of the regulatory, ergonomic, safety (as per ATEX rating [18]), installation cost, and technology maturity factors, the EPR was selected as the optimal way to automate the control of the nozzle emulator. The principle of its operation is elaborately discussed in [16], where an applied voltage control signal translates into a pneumatic output. For this application this output results in the actuation of the nozzle emulator and therefore controls the backpressure in an FMU during a test.

The design of the controller for the automation-capable actuation mechanism (i.e. the EPR) was realized using a validated model of the in-service MPR. Where the model input is a voltage instead of torque, and its output is the backpressure in the FMU. The reason for this is that, the backpressure in the FMU is the process variable that the MPR is controlled to achieve, rather than the pneumatic output of the MPR (which is not measured). Given the need for the controller to incorporate the dynamical aspects of backpressure control that can only be captured during the test of an FMU on the test rig. If a model

of the model of the EPR were the basis of the controller design, it will lack some of the fundamental dynamics that are present during the control of the FMU backpressure on the test rig.

The test specification for the control of the backpressure in an FMU requires a steady state response of 3 seconds: the time it takes an experienced human operator to perform the same task. The accuracy of the control of the backpressure is ± 10 psig of a set point, across a test range of 0 – 1240 psig [3], [7]. Although an overshoot of 30% is the norm during manual tests of an FMU, a target of10% has been specified for its automatic control. Including an oscillatory amplitude of no more than 1% of the set point.

3.1 Model of actuation mechanism

The physical structure of the MPR was decomposed into an interacting model of mass-spring and damper components, as shown in Fig. 4. It is shown that the application of a torque results in a downward force (positive) which displaces other elements of the regulator, in order to increase the orifice available to pneumatic flow, and thus increase the pneumatic force of pilot signal controlling the nozzle emulator.

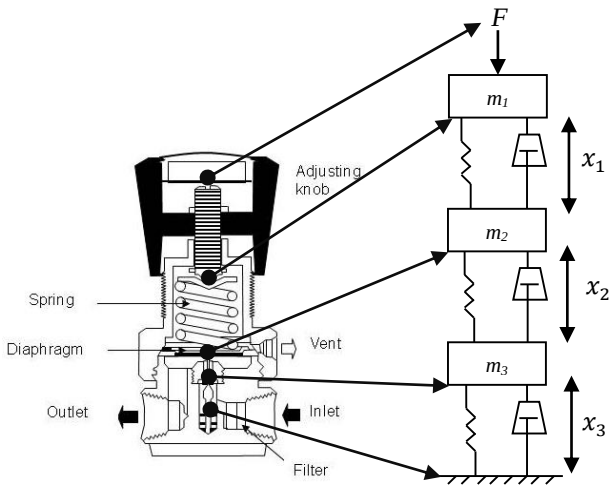

Fig. 4: Model abstraction of the MPR, the actuation mechanism of the nozzle emulator

From this abstraction, mechanical torque applied to the regulator by means of the rotation of the adjusting knob is translated into a force (*F*). This can be represented as a function of the pitch (*p*) displacement the force causes the screw threaded shaft to move through, and the radius (*R*) of the knob through which the torque (*Q*) is applied [19], [20]. This relationship is shown in Equation (1), with no friction.

$$F = Q \times \frac{p}{6.2832R} \quad (1)$$

A clockwise torque that results in this force becoming greater than the total resistive forces of the rest of the regulator elements and flow force, F_{P_2}, will cause the displacement of the mass, m_1—the ball bearing: Equation (2). The acceleration of this mass is downward and results in the displacement, x_2, of the second mass component: the diaphragm assembly, mass m_2, shown in Equation (3). The same balance of forces effect, causes the last mass element holding the orifice restriction in the regulator to move in a downward direction according to Equation (4).

$$m_1\ddot{x_1} = \left[F - k_1\,(x_1 - x_2) - c_1(\dot{x_1} - \dot{x_2}) - F_{P_2}\right] \quad (2)$$

net force — applied torque — resistive forces

$$m_2\ddot{x_2} = [\,k_1\,(x_1 - x_2) + c_1(\dot{x_1} - \dot{x_2}) - k_2\,(x_2 - x_3) - c_2(\dot{x_2} - \dot{x_3})] \quad (3)$$

$$m_3\ddot{x_3} = [\,k_2\,(x_2 - x_3) + c_2(\dot{x_2} - \dot{x_2}) - k_3x_3 - c_3\dot{x_3}] \quad (4)$$

The net (downward) force coming through from the displacement of mass m_3, will displace (by x_3), the orifice restriction of the regulator to allow more pneumatic media to flow through to the top of the nozzle emulator. The relationship between the displacement of the restriction and area available to pneumatic flow was modelled on the principle of two intersecting circles: illustrated in Fig. 5, and stated mathematically in Equation (5) [21].

$$\dot{A_{tx}} = \left[\left(-r\sqrt{4r^2 - {x_3}^2}\right) - \left(\frac{2r^2 - {x_3}^2}{\sqrt{4r^2 - {x_3}^2}}\right)\right]\frac{dx_3}{dt} \quad (5)$$

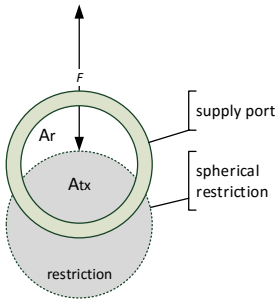

Fig. 5: Concept of orifice control in pneumatic regulator

It was assumed that the total orifice area is the same as the supply port area and the output port area, with radius, *r*. The non-linear relationship shown in Equation (5) was simplified based on the assumption that $r \gg x_3\ \forall F$: Equation (4). Equation (5) was reduced to Equation (6) below.

$$\dot{A_{tx}} = \left[(-r \times 2r) - \left(\frac{2r^2}{2r}\right)\right]\frac{dx_3}{dt} = |(-2r^2 - r)\dot{x_3}| \quad (6)$$

This area of intersection is the area not available to pneumatic media flow. Thus to get the area available to flow, A_r, the area of intersection is subtracted from the total area, A_{total}, of the orifice as given by Equation (7).

$$A_r = A_{total} - A_{tx} \quad (7)$$

However for pneumatic media to flow from the supply side to the output side, there is a pressure difference that results from a balance of forces due to the position of the orifice restriction. It is given by Equation (8), and reflects the direct relationship between the differential pressure across the regulator and the balance of forces. Where P_2 is the regulated output pressure and P_1 the pneumatic supply pressure to the MPR.

$$\Delta F = F_{x_3}$$

$$\Delta F = \Delta P \times A_r = (P_1 - P_2)A_r \quad (8)$$

$$F_{x_3} = m_3 \ddot{x_3}$$

$$\Rightarrow (P_1 - P_2)A_r = m_3 \ddot{x_3}$$

$$\therefore P_2 = P_1 - \frac{m_3 \ddot{x_3}}{A_{total} - A_{tx}} \quad (9)$$

Finally, Equation (9) shows that the pressure at the output of the MPR, is a function of the net force acting orifice restriction, initiated by the force applied mechanically. The variable F_{P_2} in Equation (2), is a function of this regulated pressure that enables the regulator to maintain a regulated pressure. For completeness, Table 1 shows the magnitudes of torques and the P_2 pressures they result to, at the control port of the nozzle emulator. These were measured using a torque wrench.

torque (lb-in)	torque (Nm)	P2 (psig)	P2 (%P1 = 464 psig)
0.2	1.77	29.0	6%
0.4	4.24	69.5	15%
1.8	15.93	261.0	56%
2.3	20.355	333.5	72%
3.2	28.32	464.0	100%

Table 1: The torque-to-regulated pressure output of an installed MPR

Although the nozzle emulator's dynamics were considered insignificant for automatic control, other characteristics had to be accounted for. In particular the linearity. It was learned that the nozzle emulator used to test the PUT has a gain factor of 1:5, i.e. for each pneumatic pressure applied, a hydraulic backpressure five times more is generated.

$$P_{hydraulic} = 5 \times P_2 \quad (10)$$

The relationship between this gain ratio of input vs. output, and the displacement of the orifice restriction of the nozzle emulator were not considered. Instead the pneumatic pressure generated by the regulator model was multiplied by five in simulation (Equation 10).

3.2 Model simulation results and validation

The model of the regulator was simulated in order to validate its representativeness of the installed one on the test rig. In order to design a feasible controller that can deliver on the test specifications, the response of the actual regulator under the control of two categories of operators was used. One operator was experienced and the response of the regulator under their control was used as the benchmark of the minimum response time the electronic controller must achieve, as a safe start point. The second operator was new on the job, and the response of the regulator was used as the maximum response time an electronic controller must not exceed to remain useful from a business perspective.

The validation of the model response was used to improve the model parameters until a satisfactory model response was achieved. In particular adjustment of the stiffness and 'damper' coefficients, for which there were no available reference values for. Other parameters such as the masses were estimated from first principle relationships. E.g. the mass of the ball bearing mass $m_1$was assumed to be a spherical steel ball. Using a reference density for steel and the volume occupied by the ball, the mass was estimated by multiplication of the density and volume. The model that was eventually used as a basis to design the PID controller gave the response shown in Fig. 6. From this response, it can be seen that the delay of the model response, in terms of the time constant in response to a set point command of 240 psig is within the band of acceptable response.

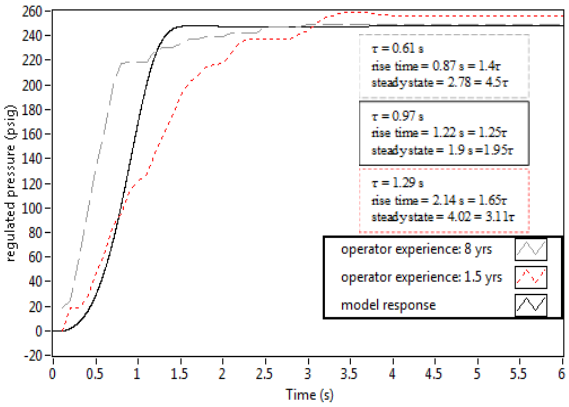

Fig. 6: Graphical validation of model response

The model also responded in a similar way to the installed MPR, giving an underdamped response at higher regulated output pressures due to leakage. This can be seen in Fig. 7.

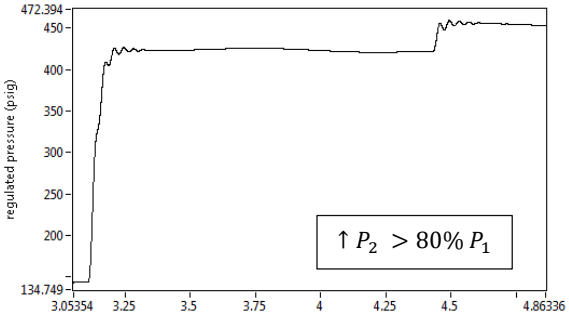

Fig. 7: Representative model response at high pressures

Eventually the model was extended to include the gain ratio of the nozzle emulator. Its response was then validated with actual measurements of the hydraulic backpressure created a PUT at higher fuel flow pressure as shown in Fig. 8.

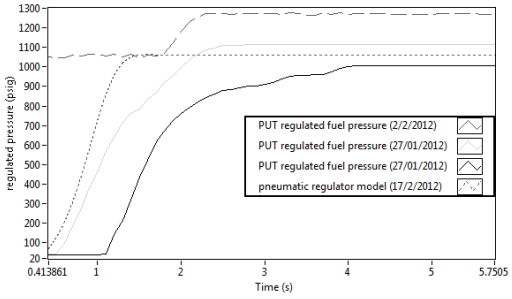

Fig. 8: Validation of complete actuation mechanism model

A graphical assessment of the abstracted model response of the nozzle emulator and its actuation mechanism show that the model is relatively representative of the response rate in particular. Given that its rate of response is almost parallel with

the rates of response measured on the test rig, on different days and under the control of different human operators.

3.3 Automatic controller design

Estimation of the PID controller gains were achieved using the reaction of the process to a step input signal, a method proposed by Nichols-Zeigler [8], [9], [12], [22]–[24].The gains determined from the process reaction (Fig. 9) are used as a start point to tune an automatic controller of the form shown in Equation (11), for the control of the nozzle emulator model.

$$u(t) = K_p\left(e + \frac{1}{T_i}\int_0^t e dt + T_d\frac{de}{dt}\right) \qquad (11)$$

The proportional action K_p, is an actual number; the integral gain is lumped as $K_i = \frac{K_p}{T_i}$, a ratio of K_p and the integral period T_i, and the derivative gain is the product of K_p and the period, T_d of the controller's derivative action

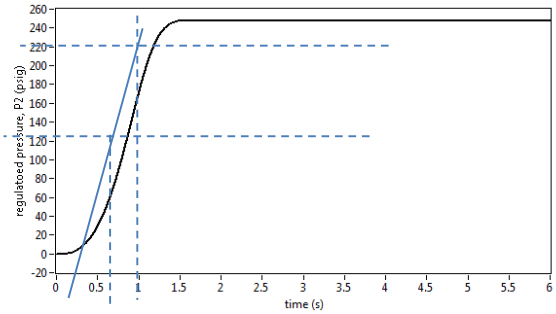

Fig. 9: Process reaction curve based on model response

$K_d = K_pT_d$. Where: u(t) is the controller output in volts and e is the difference between the desired backpressure and the actual backpressure in the FMU. The PID gains were estimated using Table 2, based on the model response to a step input equivalent to a test range of the FMU, instead of a unit step input [23].

PID	K_P	T_I	T_D
	$\frac{1.2P}{RL}$	$2L$	$0.5L$
	K_p = 2.55	= 0.8 s	= 0.2 s
		$\therefore K_i = 3.187$	$K_d = 0.51$

Table 2: PID controller tuning method

P is the set point command of 250 psig; L is the lag time, approx. 0.4 s, and R is the rate of response (equivalent to the slope of Fig. 9).

$$\therefore R = \frac{M}{\tau} = \frac{250}{0.9} \approx 294.11\ psig/s$$

Where M is the steady-state value of the backpressure in the FMU; τ is the time constant, ~0.9 s, which is equivalent to the difference between the time when the model response reached 90% of the set point command, and the time axis intersection of the maximum gradient line of the curve. Or the time at which the process reaction is at 63% of the set point commanded input. The structure of the controller in simulation is shown in Fig. 10.

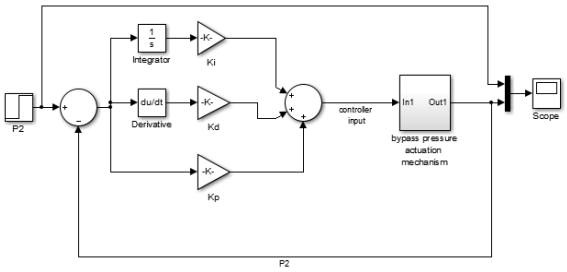

Fig. 10: Architecture of PID controller

Using a set point command of 200 psig as input into the controller model, different controller gains were used alongside those estimated from the complete actuation mechanism model. The simulation results in Fig. 11 show that the model-derived gains deliver a fast response of 1 s, with < 0.1% overshoot and no oscillation.

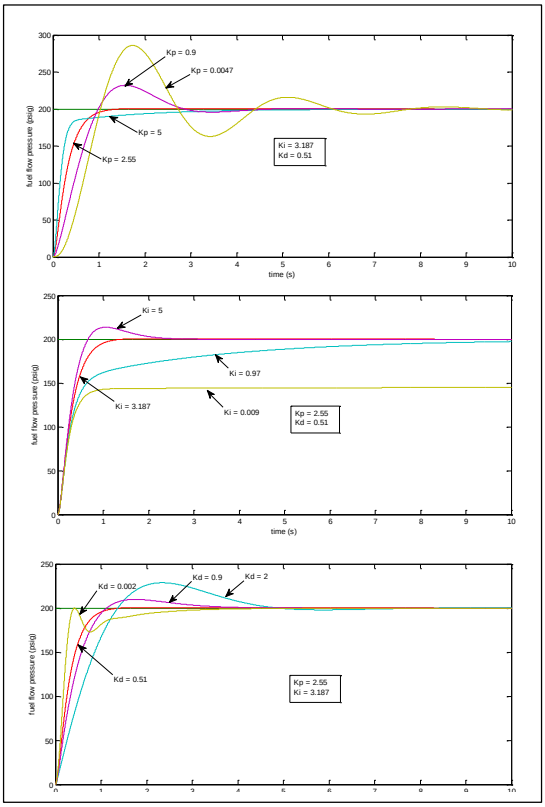

Fig. 11: Results of controller design simulation studies

An additional set of gains that delivered similar control performance, but with a slower response were selected from the simulation studies results of Fig. 12. These sets of PID gains were chosen in case the gains estimated through simulation gave process responses that were too fast for the dynamics of other components on the test rig to accommodate, or if the control performance was unsatisfactory.

A prototype system was designed and built to test the automatic control of the backpressure in the FMU. It incorporated the controller designed above, implementing the PID control law.

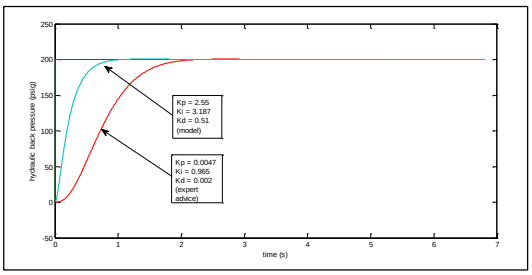

Fig. 12: Controller design simulation studies

Such that the controller controls the EPR, actuating the nozzle emulator to achieve a commanded backpressure in the FMU. Fig. 13 shows the live test set up, which is based on the schematic shown in Fig. 14.

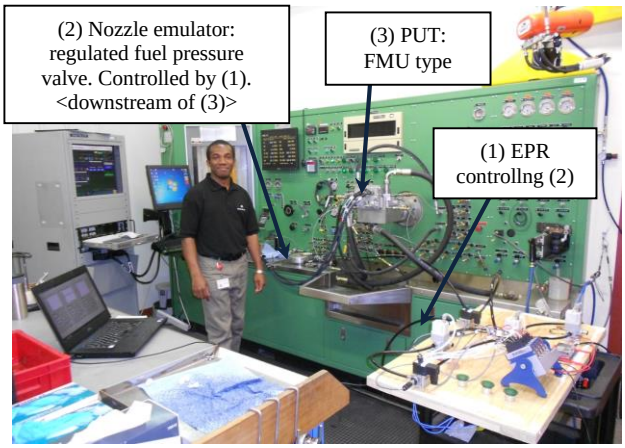

Fig. 13: Hardware-in-the-loop test of the prototype automatic control system on the nozzle emulator

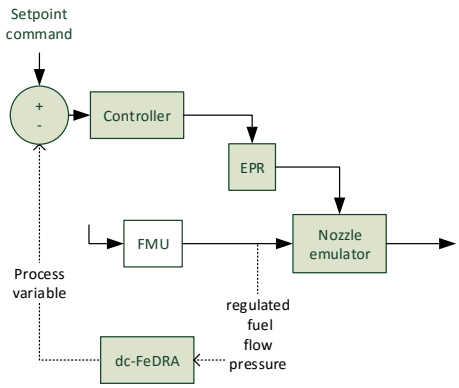

Fig. 14: Schema of the automatic control of the backpressure in an FMU

The software application was developed and run on a DELL Precision M4500 laptop computer. NI DAQMx™ drivers were installed on the computer to enable the seamless control of the EPR from software and the acquisition of data from the input modules of the NI CompactDAQ via a USB protocol [25]. The EPRs used to implement the prototype were manufactured by SMC, Part Number: ITV2050-33F4BN3-Q, with an orifice sizing rating of $C_v = 0.6$ [16]. It was estimated with the methodology discussed in [26]. The EPR was calibrated using a supply pressure of 100 psig, with a 10 V control signal range. The pneumatic media is compressed air flowing at 5 SCFM.

3.4 Hardware-in-the-Loop test results

The results from the test revealed the response time of the process is in the range of *milliseconds* not seconds (< 100 ms). It also revealed nozzle emulator having a linear gain ratio of 1:5 is non-linear. The gain is affected by the mass flowrate of the fuel during a test. So at lower fuel flows the gain ratio is linear, but changes at higher fuel flows.

These observations are summarized in Table 3. The former outcome supported the use of gains around the second choice of gains, which were smaller and accommodated the non-linear gain ratio of the nozzle emulator.

These insights of the nozzle emulator's control were incorporated into the implementation of a control application. This application has been integrated into a network of other process controllers that set up the test conditions automatically, during the test of an FMU. These have been integrated into an automation test system.

Regulated fuel pressure			
EPR output	**Backpressure (PV)**	**Inlet fuel flow**	**Identified misconception (expected)**
5 psig	5 psig	4,369 pph	Response time < 100 ms
19 psig	100 psig	2,550 pph	Response time < 100 ms
40 psig	201 psig	4,323 pph	Response time < 100 ms
70 psig	1210 psig	21,200 pph	Gain ~ *1:17.28* (1: 5) & response time < 100 ms

Table 3: Findings from hardware-in-the-loop tests of prototype

The EPR integrated into the automation system for full scale control of the backpressure was a pilot configuration with the same C_v rating as the prototype, but with a range of 0-500 psig.

4 Result and Discussion

The automatic controller for the nozzle emulator was used to step the nozzle emulator constriction across the full range of an FMU: Fig. 15. On observation of the process control response, the backpressure overshoots during step changes in the input. There is also a marginal oscillation at higher levels of fuel flow rates > 20,000 pph.

The overshoot is indicative of a high proportional gain action. It is also a symptom of an impulsive derivative action, known as the 'derivative kick'. Both of these can be improved on by further tuning of the PID gains. The later issue of marginal oscillation is believed to be caused by an insufficient integral action.

Nonetheless, the backpressure of the metered fuel inside the FMU was being achieved automatically with an acceptable control error that can be improved on.

In order to improve the controller performance, different measures were taken to minimize these undesirable aspects of the process response under the automatic controller application

for the nozzle emulator. For instance, the implementation of different PID gains across the test range of the FMU. Thus a gain switching scheme was adopted.

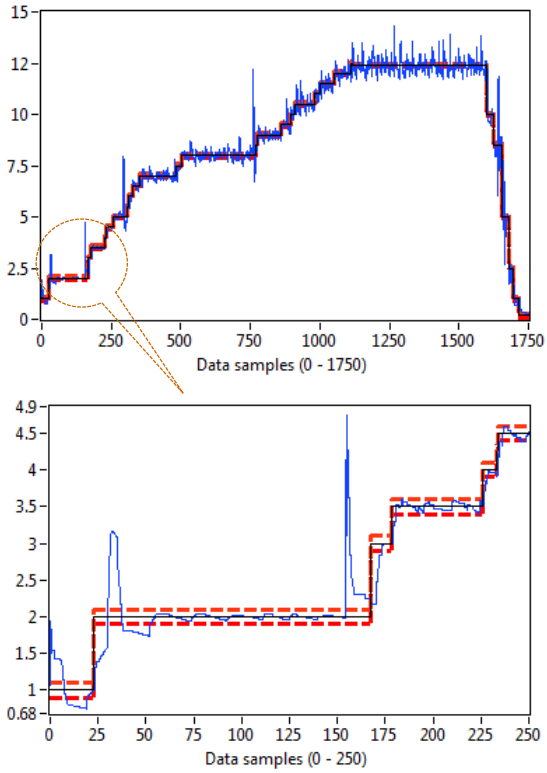

Fig. 15: Normalized backpressure reading under the automatic control of the nozzle emulator across the full test range of an FMU.

Noting that this controller would work simultaneously with other automatic controllers in a multivariable formation, it was restructured as follows:

i) the set point was processed through a first order response filter to ramp set points and thus reduce derivative kick.

ii) adapted with an anti-windup strategy to improve the steady-state error performance [27].

5 Conclusions

In this paper we have presented a classical approach to the development of an automatic process controller. Although for a process with a response faster than that observed in the process industry of ~100 mS. Such that it was integrated into an automation system for the automated test of fuel control systems used on civil transport aircraft engines.

It shows how the actuation mechanism of a nozzle emulator was automated. Including the design of the electronic controller based on a model of the installed actuation mechanism.

Fundamentally, it has demonstrated how automation of the test of a critical system was achieved in practice, thus paving the way for improvement of the automated process control performance.

Finally, our work demonstrates that the PID control law can provide the necessary level of control accuracy and is robust for this engineering process. Given the dearth of publications in the body of knowledge from this sector of civil aviation, this work serves as a basis to assess other approaches.

Acknowledgement

This project began as a Knowledge Transfer Partnership (KTP), in the U.K., January 2011 – 2013. The authors are grateful to Woodward Inc. U.K., a subsidiary of Woodward Inc. for sponsoring the project. The contributions of the Test & Product Engineering teams of Woodward Inc., USA are also duly acknowledged. Including other industry collaborators: Bauer Inc., Contrex Inc., Tescom U.K. and National Instruments U.K.

References

[1] R. Langton, C. Clark, M. Hewitt, and L. Richards, *Chapter 14: Aircraft Fuel Systems*. 2009.

[2] S. Garg, “Fundamentals of Aircraft Turbine Engine Control.”

[3] I. Azolibe, “Towards Autonomous Test of Aircraft Engine Fuel Control Systems,” no. May, pp. 1–29, 2012.

[4] Boeing, “Current Market Outlook 2015 - 2034,” 2015.

[5] Clearwater International, “GLOBAL AEROSPACE REPORT 2014 INTERNATIONAL DEALS Welcome,” 2014.

[6] IAE International, “Engine Facts | International Aero Engines,” 2015. [Online]. Available: http://iae.wpengine.com/products/engine-facts/. [Accessed: 02-Sep-2015].

[7] Woodward Governor Company, “Final Test Procedure for the V2500 FMU.” pp. 1–9, 2012.

[8] J. G. Ziegler, N. B. Rochester, and N. Y. Rochester, “Optimum Settings for Automatic Controllers,” *ASME*, 1942.

[9] A. O. Dwyer, “PI and PID controller tuning rules : an overview and personal perspective GC ,(s) = K,” pp. 161–166, 2006.

[10] S. Bennett, “Development of the PID Controller,” *IEEE Control Syst.*, 1993.

[11] M. Zhuang and D. P. Atherton, “Automatic tuning of optimum PID controllers,” 1993, vol. 140, no. 3, pp. 216–224.

[12] K. . Astrom and T. Hagglund, *PID Controllers: Theory, Design, and Tuning.*, 2nd ed. 1995.

[13] Z. M, “Computer Aided {PID} Controller Design,” no. July, 1992.

[14] R. Isermann and P. Automation, “TRENDS IN THE APPLICATION OF MODEL-BASED FAULT DETECTION AND DIAGNOSIS OF TECHNICAL PROCESSES,” vol. 5, no. 5, pp. 709–719, 2000.

[15] R. Isermann, *Fault-Diagnosis Systems: An Introduction from Fault Detection to Fault Tolerance*. Springer, 2006.

[16] SMC, “Electro-Pneumatic Regulator.” 2004.

[17] Tescom, “ER3000 Training.” 2012.

[18] HSE U.K, “ATEX and explosive atmospheres - Fire and explosion,” 2015. [Online]. Available: http://www.hse.gov.uk/fireandexplosion/atex.htm. [Accessed: 13-Sep-2015].

[19] E. Oberg, F. D. Jones, H. L. Horton, and H. H. Ryffel, *Machinery ’ s Handbook*, 28th ed. New York: Industrial Press, 2008.

[20] E. Oberg and F. D. Jones, *Machinery’s Handbook for Machine Shop and Drafting-Room*. New York: Machinery Publishing Co. Ltd, 1944.

[21] E. W. Weisstein, “Circle-Circle Intersection,” 2015. [Online]. Available: http://mathworld.wolfram.com/Circle-CircleIntersection.html. [Accessed: 13-Sep-2015].

[22] F. Peacock, “PID Tuning Blueprint,” 2008, p. 69.

[23] W. Bolton, *Mechatronics: Electronic Control Systems in Mechanical & Electrical Engineering*, Fifth. London: Pearson, 2011.

[24] K. J. Åström, W. S. Levine, and T. Hägglund, “PID Control,” in *The Control Handbook*, IEEE Press, 1996, pp. 198–209.

[25] National Instruments, “What Is CompactDAQ?,” 2015. [Online]. Available: http://www.ni.com/compactdaq/whatis/. [Accessed: 30-Aug-2015].

[26] Fisher Controls International LLC, *Control Valve Handbook*, Fourth. 2005.

[27] K. H. Ang, G. C. Y. Chong, and Y. Li, “PID control system analysis, design, and technology.,” *IEEE Trans. Control Syst. Technol.*, vol. 13, no. 4, pp. 559–576, 2005.